



Pergamon

SCIENCE @ DIRECT®

Tetrahedron: *Asymmetry* 14 (2003) 2433–2444

TETRAHEDRON:
ASYMMETRY

Molecular basis of the Cotton effects induced by the binding of curcumin to human serum albumin

Ferenc Zsila,* Zsolt Bikádi and Miklós Simonyi

Department of Molecular Pharmacology, Institute of Chemistry, Chemical Research Center, POB 17,
H-1525 Budapest, Hungary

Received 23 May 2003; accepted 16 June 2003

Abstract—Curcumin binding to human serum albumin (HSA) has been found recently to induce bisignate CD curves due to intramolecular exciton coupling between the two feruloyl chromophoric parts. The present study reports further results on this interaction. UV–vis and chiroptical properties of HSA-bound curcumin were analyzed in detail by comparison with bilirubin–albumin complexes. Data obtained by UV–vis and fluorescence spectroscopy, CD displacement experiments and molecular modelling methods suggested the primary binding site of curcumin to be located in site I of HSA. Since acid–base dissociation of the polyphenol type curcumin molecule plays a fundamental role in albumin binding, light absorption spectra of curcumin and half-curcumin (dehydrozingerone) were studied in ethanol and in water at different pH values. It is established that the phenolic OH group of curcumin is the most acidic and that its dissociation is responsible for both the large red-shift of the main absorption band and the binding of curcumin to HSA in a right-handed chiral conformation. Additionally, it is demonstrated that pH dependent induced CD spectra can be utilized to determine the acid–base dissociation constant; from chiroptical data the first pK_a value of curcumin was calculated (8.28).

© 2003 Elsevier Ltd. All rights reserved.

1. Introduction

Curcumin, the main yellow pigment of the powdered rhizome (turmeric) of the perennial herb *Curcuma longa* L. has been used for centuries as a spice and food coloring agent.¹ In the Indian subcontinent and Southeast Asia, turmeric has traditionally been used to treat many diseases including inflammation, skin wounds, and tumors.² Recently, curcumin has attracted much interest because several experimental studies have demonstrated that this natural polyphenol has anti-inflammatory, antineoplastic and anti-angiogenic activities.^{3,4} To exert its beneficial effects curcumin has to be transported to cells. So, distribution and bioavailability of curcumin may be influenced significantly by its interaction with serum proteins.⁵ In a previous communication we reported that binding of curcumin to human serum albumin (HSA) can sensitively be studied by circular dichroism (CD) spectroscopy.⁶ The weak, induced CD spectrum of

curcumin–HSA complex measured at physiological pH profoundly changes upon alkalization showing an oppositely signed CD band pair according to the visible absorption band of curcumin. This induced optical activity was attributed to a bent, right-handed chiral conformation of the HSA-bound curcumin molecule in which feruloyl chromophores interact with each other via chiral exciton coupling.

Curcuminoids and their derivatives are the subject of growing interest in human medicine⁷ but their rational and successful application should rely on the mechanism of action at the molecular level. In order to gain a better understanding in physico-chemical properties of curcumin governing its spectral behavior and to draw relevant conclusions on the curcumin–HSA binding mechanism, additional CD and absorption spectroscopic measurements were performed on half-curcumin, curcumin and the curcumin–HSA complex. Our results provide a starting point for studying interactions of curcumin with different, potential targets, i.e. enzymes and nucleic acids.⁸ Additionally, as a new optical probe on HSA, curcumin is useful to provide further insight into ligand binding properties of this protein.

* Corresponding author. Fax: (+36) 1-325-7750; e-mail: zsferi@chemres.hu

2. Results and discussion

2.1. UV–vis absorption spectra of half-curcumin in ethanolic and aqueous solutions

Before attempting to interpret spectroscopic characteristics of the curcumin–HSA complex, it is of vital importance to investigate and understand the electronic absorption spectrum of curcumin itself. Formally, curcumin (diferuloylmethane) consists of two symmetrical parts joined by a methylene bridge (Fig. 1). Therefore, it is reasonable to study first the simple dehydrozingerone molecule (Fig. 1) called as half-curcumin (hC), a close analog of ferulic acid.¹² The hC molecule contains a donor–acceptor type chromophore¹³ where the electron donating groups (-OH and -OCH₃) are linked to the electron accepting carbonyl part by an unsaturated bridge. Between 270 and 450 nm hC shows an intense band in the near-UV region with a shoulder around 300 nm (Fig. 2). This band corresponds to an electronic dipole allowed π - π^* , intramolecular charge-transfer transition. Similar to structurally related compounds such as *p*-dimethylamino- and *p*-methoxycinnamate,^{14,15} the electronic transition dipole moment of hC is presumably polarized along the long axis of the molecule. Figure 3a illustrates HOMO–LUMO of the simplified hC molecule while Figure 3b shows the calculated changes in the π -electron density accompanying electronic excitation to the first excited state. Both the

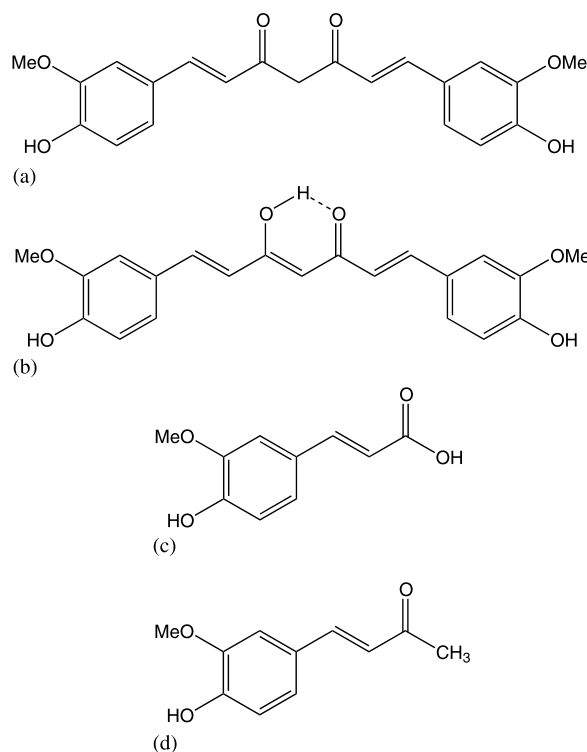


Figure 1. Chemical structures of keto (a) and enol (b) forms of curcumin [1,7-bis(4-hydroxy-3-methoxyphenyl)-1,6-heptadiene-3,5-dione], ferulic acid (c) [3-(4-hydroxy-3-methoxyphenyl)-2-propenoic acid] and dehydrozingerone (d) [half-curcumin; 4-(4-hydroxy-3-methoxyphenyl)-3-buten-2-one].

qualitative and quantitative pictures clearly prove a net flow of electron density (intramolecular charge transfer) from the benzene ring to the carbonyl moiety. Since a large π -electron deficiency arises at the *para* position, attaching an electron donor group here stabilizes the excited state and lowers its energy relative to the ground state, resulting in the bathochromic shift of the corresponding absorption band. Electron donor strength of hydroxyl substituents can greatly be enhanced by the action of a base.^{16–18} Accordingly, a strong red shift was seen upon addition of a small volume of KOH to the ethanolic solution of hC (Fig. 2). Increased in intensity, the principal absorption band moves into the visible region (340.2→417.2 nm; $\Delta\sigma = 5425 \text{ cm}^{-1}$) and the sample becomes yellow coloured. Analogous changes were observed in alkaline aqueous environment as well; going from pH 7.4 Ringer buffer to pH 9.0 Tris–HCl buffer solution, the absorption maximum of hC shifts from 337.8 nm to 395.4 nm ($\Delta\sigma = 4312.5 \text{ cm}^{-1}$, not shown). These results clearly prove that deprotonation of the *p*-hydroxy group is responsible for the extensive spectral changes and predict curcumin to behave likewise in alkaline solution.

2.2. UV–vis absorption spectra of curcumin in ethanolic and aqueous solutions

It is well documented that, due to its β -diketone moiety, curcumin exists entirely in the enol form with a *trans*-geometry both in solid state¹⁹ and solution^{20–22} (Fig. 1). Thus, in this planar geometry the π -systems of the two feruloyl chromophores are allowed to interact with each other via the central, sp^2 -hybridized carbon atom resulting in a common conjugated π -system.^{12,23} Yellow coloured ethanolic solutions of curcumin exhibit an intense, round-shaped absorption band cen-

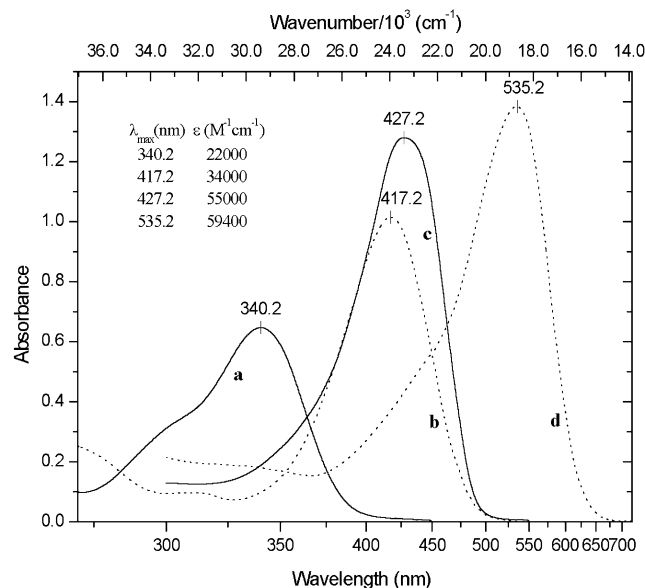


Figure 2. UV–vis absorption spectra of half-curcumin (a, b) and curcumin (c, d) obtained in EtOH (solid lines) and EtOH+KOH (dotted lines) solutions. Inset shows molar absorption coefficients (ϵ) in M⁻¹ cm⁻¹ ($c_{\text{curcumin}} = 2.3 \times 10^{-5}$, $c_{\text{hC}} = 3.0 \times 10^{-5}$ M; cell length 1 cm; $t = 25^\circ\text{C}$).

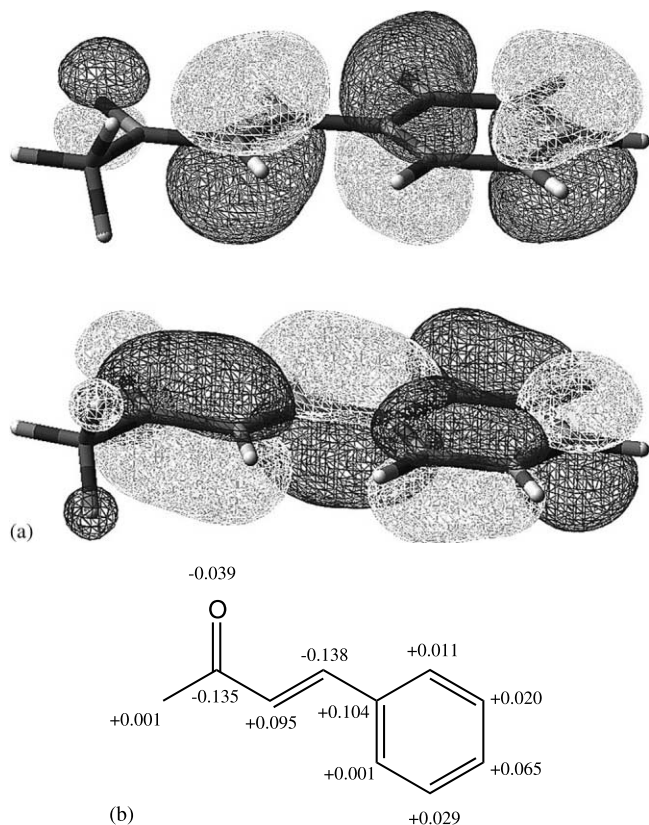


Figure 3. (a) Frontier molecular orbitals (HOMO and LUMO, *A* and *B*) of 4-phenyl-3-buten-2-one molecule geometrically optimized by Gaussian 98 program. (b) First excited state differential atomic charges of 4-phenyl-3-buten-2-one molecule. Positive signs indicate a decrease and negative signs an increase in π -electron density upon electronic excitation to the first excited state (semiempirical calculation was performed by using MOS-F).

tered at 427.2 nm (Fig. 2); in apolar solvents, i.e. in benzene, this band shows a characteristic vibrational fine structure which resembles the spectra of fully conjugated linear molecules such as carotenes and carotenoids.¹² It should be emphasized that the visible absorption band of curcumin stems from a $\pi \rightarrow \pi^*$ transition and not from an $n \rightarrow \pi^*$ one as stated by Balasubramanian based on theoretical calculations.²⁴ Most likely, the weak, electronic dipole forbidden $n \rightarrow \pi^*$

band is located somewhere under the main absorption band. Based on experimental data, several investigators suggested the first excited state of curcumin is highly polar due to intramolecular charge transfer from the phenyl ring towards the carbonyl moiety.^{12,22,23} This conclusion is in good agreement with our semiempirical calculations (Fig. 4) showing the displacement of negative charge to the centre of the molecule. The calculated difference charge values show that, in a given molecule at a given moment, there is a significantly larger charge deficiency on one aromatic ring than on the other, especially in the *para* and *meta* positions. Additionally, this picture suggests that the dissociation of one phenolic OH group may be sufficient to produce a bathochromic shift of the main absorption band via stabilization of the first excited state.

Similar to hC, alkalization changes dramatically the light absorption properties of curcumin; upon addition of KOH to its ethanolic solution the main visible band shifts from 427.2 nm to 535.2 nm ($\Delta\sigma = 4723.6 \text{ cm}^{-1}$) and the sample shows a stable purple color. Very similar spectral changes were reported in the literature obtained by addition of NaOH to curcumin dissolved in mixtures of methanol/water (1:1) and dioxane/water (3:1).^{25,26} Above pH 7 in pure aqueous solution, however, free curcumin molecules are very unstable and undergo rapid hydrolytic degradation with a half-life of a few minutes accompanied by a strong decrease of the absorbance values in the visible region.^{27,28}

The above discussion on the excited state properties of hC and curcumin molecules strongly suggests the crucial role of ionization of *p*-hydroxy substituents in the large red shift of the main absorption band. In Table 1, UV-vis spectral data of several curcumin analogues²⁵ and related compounds²⁹ are presented to obtain better insight into the effect of the dissociation of enolic and phenolic OH groups on the absorption spectrum. These data indicate that the wavelength position of the absorption maximum is only slightly affected by deprotonation of the enolic OH (16 and 12 nm red shift). On the other hand, it is obvious that the presence of a hydroxyl group in the *para* position is essential to observe a large bathochromic shift in the absorption spectrum. Additionally, Table 1 shows that deprotonation of one phenolic OH group already produces a large red shift and the presence of a second hydroxyl

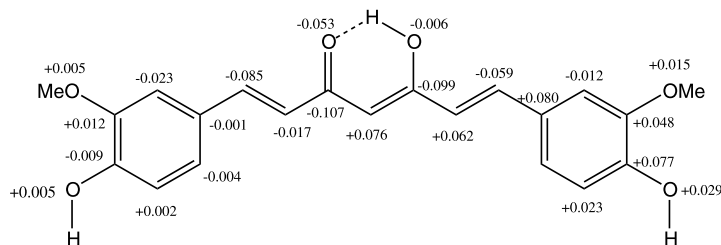


Figure 4. Differential atomic charges of curcumin molecule in the first excited state. Positive signs indicate a decrease and negative signs an increase in π -electron density upon electronic excitation to the first excited state (semiempirical calculation was performed by using MOS-F).

substituent has a minor additional influence on the absorption maximum. Thus, in agreement with the result of our quantum-chemical calculation presented above (see also Fig. 4), it can be concluded that the dissociation of one phenolic hydrogen in curcumin is almost entirely responsible for the red shift obtained by alkalization.

Since acidic dissociation of curcumin largely determines its binding mode to HSA, it is necessary to know the exact pK_a values of both the phenol and enol groups in aqueous solution. Various papers report acidic dissociation constants of curcumin but, unfortunately, these are conflicting data. Table 2 displays pK_a values of curcumin (and some related compounds) found by several authors.^{18,25,26,30–32} As can be seen, quite different assignments have been made depending on the solvent and method used. In some cases the first dissociation constants obtained by spectrophotometric titration were assigned to the enolic hydrogen^{26,30} which is a very doubtful conclusion since spectral changes measured upon alkalization are due to the deprotonation of phenol and not the enol group (see above). In smaller molecules structurally related to curcumin, phenolic dissociation constants are varied between 8.2 and 8.7 in water (Table 2). Taken together, the most likely value of the first phenolic dissociation constant of curcumin in water is between 8.0 and 8.5.

2.3. Optical properties and acid dissociation of HSA-bound curcumin molecules

Curcumin shows a weak induced CD spectrum around pH 7.4 and below^{5,6} but upon alkalization a typical, oppositely signed CD band pair evolves the amplitudes of which increase gradually with the pH values of the solution (Fig. 5). The bisignate nature of these CD spectra is very characteristic of chiral exciton interactions and the finding that the induced CEs match with the spectral position of the highly broadened and red shifted absorption band of curcumin supports further the exciton mechanism.³³ Furthermore, it would be impossible to obtain exciton CD bands if curcumin molecules bound to HSA in a planar conformation. So, the conclusion must be drawn that curcumin acquires a non-planar conformation, its two halves being twisted relative to each other at the protein binding site. Around pH 7.4 undissociated curcumin molecules predominate in the solution and bind to HSA with a planar conformation. As the CD spectra suggest, with increasing pH more and more curcumin molecules dissociate and the ionized species bind to HSA in a chiral conformation. However, there are two kinds of acidic hydrogens on curcumin, phenolic and enolic, which dissociate above pH 7.4 (Table 2). The behavior of the absorption spectrum of curcumin–HSA complex can be explained by the ionization of both phenolic sub-

Table 1. UV–vis spectroscopic data of various curcuminoids and related compounds

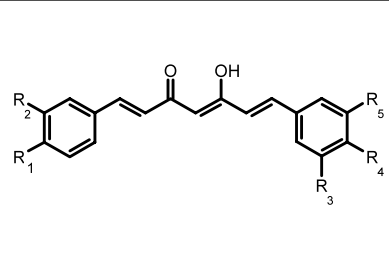
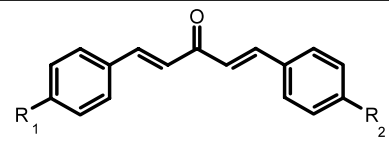
	UV/Vis absorption maximum ²⁵ (nm)		$\Delta\sigma$ (cm^{-1})
	Dioxane/Water 75% v/v	Dioxane/Water 75% v/v + NaOH	
$R_1 = R_2 = R_3 = -H$; $R_4 = -OAc$, $R_5 = -OCH_3$	399	415	+966.3
$R_1 = R_2 = -H$; $R_3 = R_4 = R_5 = -OCH_3$	405	417	+710.5
$R_1 = R_2 = -H$; $R_3 = R_5 = -OCH_3$ $R_4 = -OH$	419	481	+3076.3
$R_1 = -OH$, $R_2 = -H$; $R_3 = -OCH_3$ $R_4 = -OH$, $R_5 = -H$	423	493	+3356.7
	UV/Vis absorption maximum ²⁹ (nm)		$\Delta\sigma$ (cm^{-1})
	EtOH	0.1 M NaOH	
$R_1 = -OH$, $R_2 = -H$	364	440	+4745.2
$R_1 = R_2 = -OH$	380	470	+5039.2

Table 2. Collected literature data of acid dissociation constants of curcumin and some related compounds

Compounds	pK_a			Solvent	Method	Ref.
	Phenol 1	Phenol 2	Enol			
Curcumin	8.55	9.05	7.75–7.80	Aqueous buffer (t=31.5°C)	pH-dependent hydrolytic degradation profile	27
	–	–	7.9	EtOH-buffer 1:1	Spectrophotometric titration	30
	8.10	10.15	–	Water (t=20°C)	Spectrophotometric titration	31
	10.82	11.60	13.44	Dioxane/water 75% v/v (t=25°C)	Potentiometric titration	25
	8.89	9.76	12.28	EtOH/water 50% v/v (t=25°C)	Potentiometric titration	25
	9.30	10.69	8.54	MeOH/water 50% v/v (t=25°C)	Potentiometric titration	26
–	–	8.7	MeOH/water 50% v/v (t=25°C)	Spectrophotometric titration	26	
Diacetyl-curcumin	–	–	8.75	MeOH/water 50% v/v (t=25°C)	Potentiometric titration	26
<i>trans-p</i> -Coumaraldehyde	8.2–8.3	–	–	Water	Potentiometric titration	18
Ferulic acid	8.71	–	–	Water (t=25°C)	Potentiometric titration	32
<i>p</i> -Coumaric acid	8.73	–	–	Water (t=25°C)	Potentiometric titration	32

stituents. As mentioned, when ionized curcumin binds to HSA its two halves rotate around the central methylene group. Such rotation, however, decreases or completely cancels π -conjugation between the two feruloyl parts, so the absorption maximum should shift below 400 nm, as in the case of curcumin derivatives bearing a bulky substituent at the central methylene atom.³⁴ In spite of this, the absorption band of HSA-bound curcumin shifts to higher wavelengths which is possible only if a phenolic proton dissociates and this effect overcompensates for decreasing of the π -conjugation. Experimental manifestation of the increasing proportion of such molecules is a new absorption band around 483 nm (Fig. 5) that together with the CEs, becomes more and more intense as the pH value increases. Finally, since the intramolecular twist makes the feruloyl parts independent of each other, pK_a values of their phenol substituents become similar and we obtain a composite molecule having two, covalently attached, ionized hC chromophores.

In the light of the above, there is a direct relation between the magnitudes of induced CEs and the ratio of the phenolate species of curcumin. Therefore, CD data can be used to calculate the first phenolic dissociation constant of curcumin. Indeed, band intensities plotted against actual pH values of the solution give a typical acid–base titration curve (Fig. 6) from which the pK_a value is 8.28 (Table 2).

Regarding the interaction of curcumin with the albumin binding site, it has to be noted that dissociated ligand molecules lose their hydrogen donor properties but, at the same time, they become more powerful proton acceptors ready to form H-bonds with basic residues of HSA. Thus, due to secondary chemical interactions between the ligand and its protein microenvironment, dissociated curcumin accommodates to its

binding site as a chiral conformer. It is well known that the tertiary structure of albumin molecule is sensitively influenced by physical-chemical factors such as the hydrogen ion concentration of the solution. In the range of pH 6–9, HSA undergoes a conformational change, referred to as the neutral-base (N-B) transition.^{9,35,36} During this transition, tertiary structures of

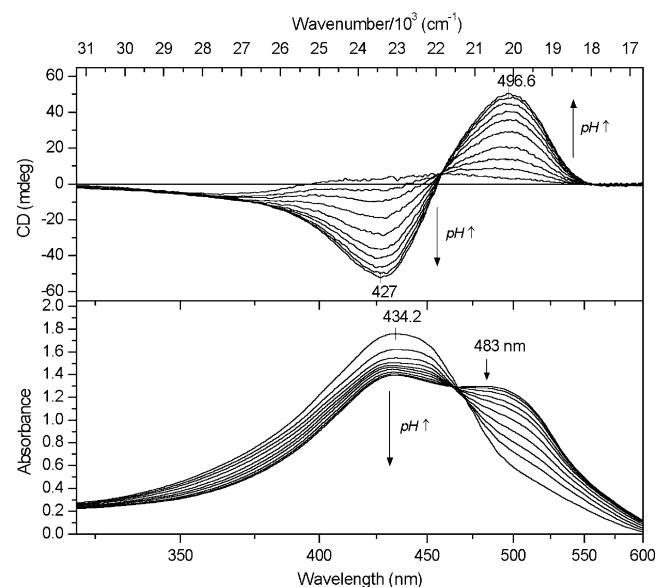


Figure 5. pH dependence of the CD and UV–vis spectra of curcumin–HSA complex formed in distilled water. CD and absorption spectra were obtained through a titration procedure adding μ l volumes of 0.01 and 0.1 M NaOH to the equimolar mixture of curcumin–HSA solution (cell length 1 cm; $c_{\text{HSA}} = 4.7 \times 10^{-5}$ M, $c_{\text{curcumin}} = 4.8 \times 10^{-5}$ M; room temperature). The pH values applied are: 6.91, 7.38, 7.68, 7.97, 8.31, 8.57, 8.78, 9.00, 9.19 and 9.32 (figure was taken from ref. 6 by permission from the publisher).

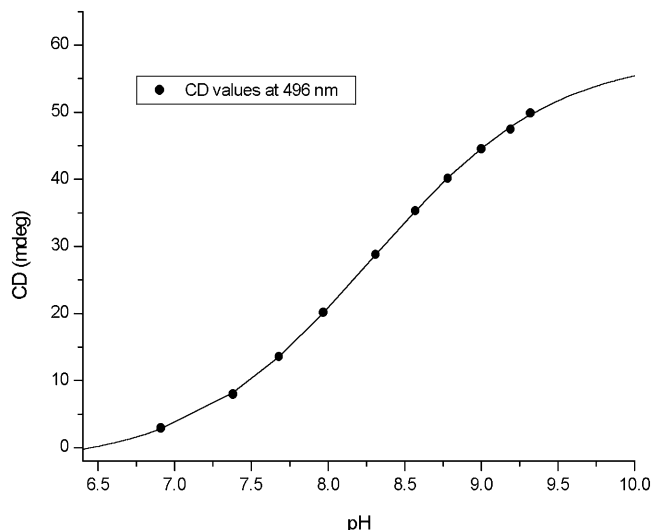


Figure 6. CD–pH titration of curcumin–HSA complex in distilled water at room temperature. Intensities of the induced positive CD band are plotted versus the pH. Circles: experimental data points; solid line: result of a curve-fitting procedure.

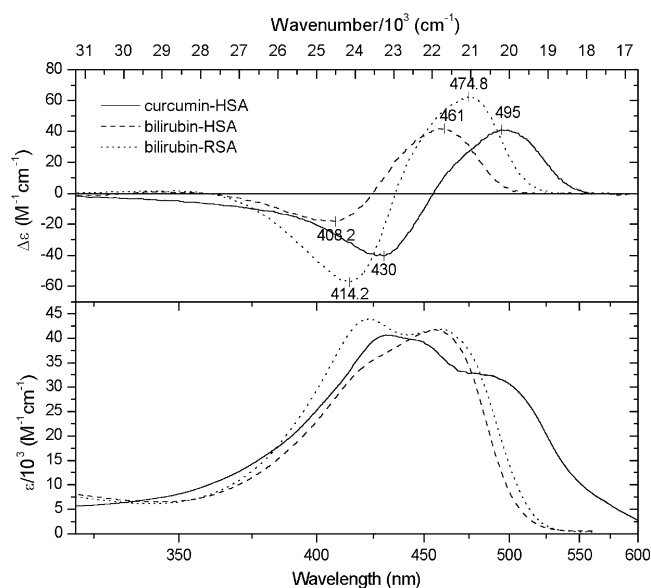


Figure 7. Comparison of induced CD and UV–vis spectra of curcumin–HSA, bilirubin–HSA and bilirubin–RSA complexes measured in 0.1 M pH 9 Tris–HCl buffer and in pH 7.4 Ringer buffer, respectively (cell length 1 cm, $t=20^{\circ}\text{C}$, $c_{\text{HSA}}=c_{\text{RSA}}=1\times 10^{-4}$ M, $c_{\text{curcumin}}=c_{\text{bilirubin}}=3\times 10^{-5}$ M)

domain I and II are modified, whereas domain III shows minimal alteration.^{9,37} At pH 6, HSA entirely exists in the N conformation, while at pH 9 the B form essentially dominates. Since binding of a given ligand to the N or B forms of HSA may be different^{38,39} the question arises as to whether the N–B transition of HSA is responsible for the bisignate CD spectrum of curcumin. However, experimental facts do not support this assumption. The N–B transition begins at pH 6 but exciton CD bands appear only above pH 7.4. Further-

more, if the N–B transition would account for the positive–negative CEs then CD intensities should reach a plateau between pH 8.5 and pH 9 but the curve in Figure 6 shows that it is not the case.

Despite of the rapid decomposition of free curcumin molecules obtained in aqueous solutions above pH 7,^{27,28} neither the shape nor the intensity of the absorption and CD bands of HSA-bound curcumin change at 20 and 37°C for several hours suggesting curcumin to be complexed in a deep, hydrophobic cavity of the protein inaccessible for water molecules. It should be noted that HSA also preserves structural integrity of curcumin molecules at physiological pH.⁵

2.4. Comparative analysis of the visible absorption spectrum of curcumin–HSA and bilirubin–albumin complexes

In pH 8.3 aqueous solution, 50% of curcumin molecules are neutral and 50% are ionized. Since the two species absorb light at different wavelengths (Fig. 2), their coexistence contributes to the broadening of the visible absorption band due to partial spectral overlap (Fig. 5). However, there is another effect that influences the absorption band of HSA-bound curcumin, namely the intramolecular exciton coupling of the feruloyl chromophores. Its action can be better studied by comparison of CD and absorption spectra of curcumin–HSA and bilirubin–albumin complexes. Induced optical activity of HSA complexed bilirubin has been studied thoroughly for many years and it is well known that the preferential binding of one chiral conformational enantiomer of this pigment is responsible for bisignate Cotton effects.^{40,41} Spectra displayed in Figure 7 demonstrate close similarity both in shape and intensity of the induced CD bands of curcumin and bilirubin supporting the above conclusion on the binding of curcumin molecules in a dissymmetric conformation. Bandwidths measured at the half-maxima of the longest-wavelength CEs of these complexes are in excellent agreement; 2250 cm^{-1} for curcumin–HSA, 2231 cm^{-1} for bilirubin–HSA and 2181 cm^{-1} for bilirubin–RSA complexes, respectively. In marked contrast, the absorption band of curcumin is much broader than that of bilirubin. As known, the long-wavelength absorption band of bilirubin contains at least two unresolved bands separated by ca. 2500 cm^{-1} which can be explained by in-phase and out-of-phase excitonic coupling between the electronic transition moments of the dipyrinone chromophores.⁴² Such splitting of the absorption band is clearly shown in the case of the bilirubin–RSA complex where the two peaks are partially resolved and their wavelength positions match with the extrema of the corresponding CD bands (Fig. 7). Thus, it is reasonable to assume that exciton splitting between electronic transition moments of the rotated feruloyl parts of HSA-bound curcumin molecules also contributes to the broadening of the main visible absorption band. So, coexistence of the split absorption band of the ionized and the absorption band of neutral molecules results in the experimental spectrum. To demonstrate how this spectral mixing

occurs, UV–vis spectrum of curcumin–HSA solution taken at pH 8.3 was approximated as the sum of the absorption curve of neutral curcumin molecules measured in EtOH and a hypothetical split band representing the protein bound ionized species (Fig. 8). In accordance with the exciton theory,³³ it was found that peak positions of the calculated split curve match well with the extrema of the corresponding CD bands (cf. Fig. 7).

2.5. CD and UV–vis spectroscopic investigation of half-curcumin–HSA interaction

In contrast to induced CD curves of curcumin, hC molecules do not show CD bands at pH 9 despite the presence of HSA; at pH 7.4 only a weak, single negative CE appears around 350 nm according to the absorption band of hC ($\Delta\epsilon_{347\text{nm}} = -1.7 \text{ M}^{-1} \text{ cm}^{-1}$, $\epsilon_{339.2 \text{ nm}} = 17000 \text{ M}^{-1} \text{ cm}^{-1}$; spectra not shown). On one hand, this result indicates that the whole diarylheptanoid structure is essential to obtain the bisignate CD bands. On the other hand, it suggests that the curcumin molecule binds in a large cavity rather than in smaller, adjacent pockets which would accommodate two halves of the ligand separately. The narrow, hydrophobic, fatty acid binding channels of subdomain IIIA located in close proximity to each other⁴³ are an example for the latter.

2.6. Probing the binding site of curcumin on HSA by ligand displacement experiments

The finding that the curcumin–HSA complex exhibits induced a CD couplet in the visible spectral region

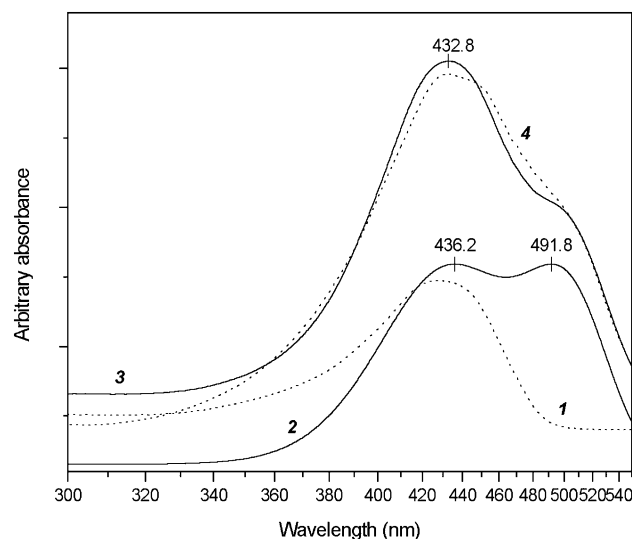


Figure 8. Reconstruction of the experimental absorption band of curcumin measured in HSA solution at pH 8.3. Ethanol absorption curve (1, dotted line) of curcumin was used to represent the unbound, neutral fraction of ligand molecules while the sum of two Gaussian bands (2, solid line) is the contribution of the dissociated, excitonically coupled albumin-bound species. The resulted (3, solid line) and experimental curves (4, dotted line) are in good coincidence.

provides a sensitive tool for studying the binding location of curcumin on HSA. In the presence of a compound having the same binding site as curcumin, amplitudes of the induced CEs should decrease due to competition. Therefore, CD displacement experiments were performed using palmitic acid, *rac*-ibuprofen, diazepam and *rac*-warfarin of which high-affinity binding sites are known on HSA. X-Ray studies revealed that the two major drug binding sites of HSA named site I and site II are located in subdomain IIA and IIIA.^{44,45} The anticoagulant drug warfarin and ibuprofen, a nonsteroidal anti-inflammatory agent, are considered as marker ligands of site I and site II, respectively.^{46,47} Ibuprofen binds to site II with $K_a = 2.7 \times 10^6 \text{ M}^{-1}$ although it partially displaces warfarin too,⁴⁸ whereas warfarin binds to site I with $K_a = 3.3 \times 10^5 \text{ M}^{-1}$.⁹ Primary binding location of diazepam on HSA is site II in subdomain IIIA ($K_a = 3.8 \times 10^5 \text{ M}^{-1}$,⁹) but a secondary binding site has also been reported in domain I.⁴⁷ Apparent binding constant of curcumin to HSA was found to be $\approx 1 \times 10^5 \text{ M}^{-1}$.⁵ Palmitic acid binding sites of HSA have recently been determined by X-ray crystallographic measurements.⁴⁶ The high-resolution structure revealed seven, asymmetrically distributed sites across all three domains of HSA, and three of them overlap with the two primary drug-binding sites in subdomains IIA and IIIA.

Addition of the above ligands to sample solutions containing curcumin and HSA decreased the magnitudes of the induced CD bands (Fig. 9). Palmitic acid turned out to be the most effective displacer followed by ibuprofen and warfarin but diazepam showed a considerably weaker displacing effect. Parallel with the

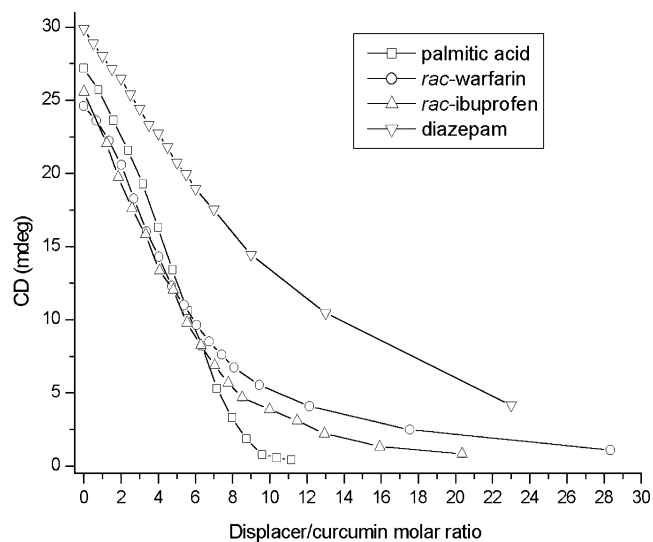


Figure 9. Results of CD displacement experiments performed with palmitic acid, *rac*-warfarin, *rac*-ibuprofen and diazepam on curcumin–HSA complex in 0.1 M pH 9 Tris–HCl buffer solution ($l = 1 \text{ cm}$, $t = 37^\circ\text{C}$, $c_{\text{curc.}} = 2.5 \times 10^{-5} \text{ M}$, $c_{\text{HSA}} = 4.9 \times 10^{-5} \text{ M}$ and $5.5 \times 10^{-5} \text{ M}$ (for diazepam)). Displacers were added as μl aliquots of ethanolic stock solutions. Positive induced CD values measured at 497 nm are plotted against displacer/curcumin molar ratios (for further details see Materials and methods).

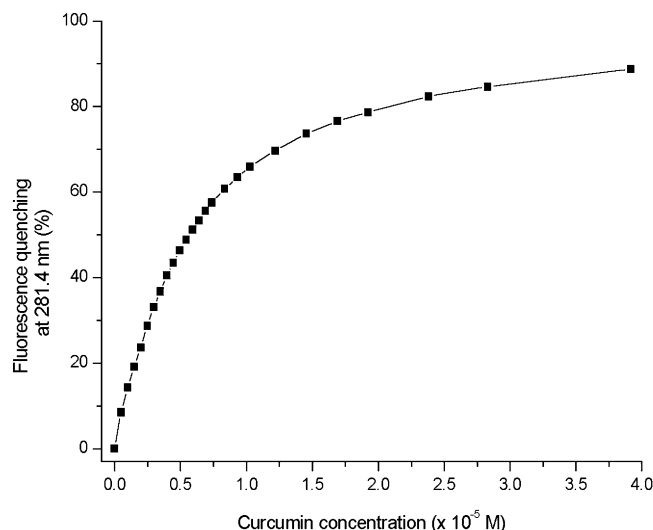


Figure 10. Fluorescence quenching of HSA by curcumin measured in 0.1 M pH 9 Tris–HCl buffer solution at 20°C. Initial and final concentrations of HSA were 4.4×10^{-6} M and 4.1×10^{-6} M, respectively. Curcumin/HSA molar ratio was varied between 0.11 and 9.66.

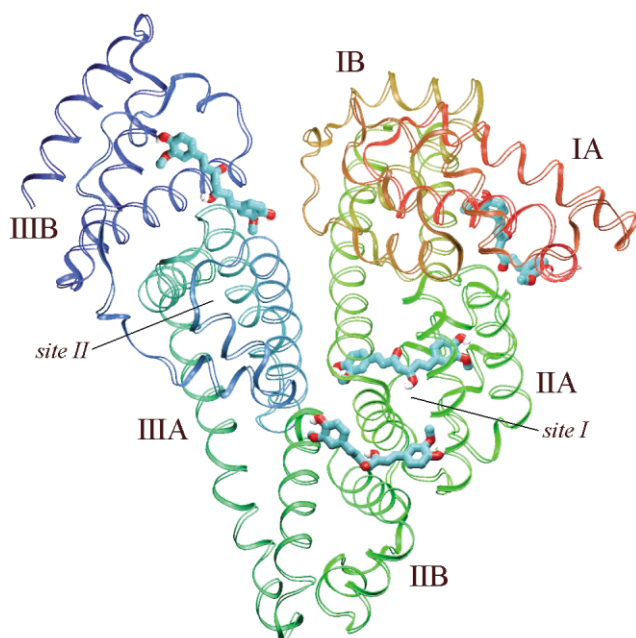


Figure 11. X-Ray crystallographic structure of HSA with curcumin molecules obtained by docking procedure. Subdomains and the two primary drug-binding sites of HSA are indicated.

decreasing CD values, palmitic acid, warfarin and ibuprofen strongly, while diazepam only slightly, reduced the absorption band intensity of curcumin suggesting displacement of curcumin by the former ligands from the binding cavity and, consequently, its hydrolytic decomposition (data not shown). These results suggest that one of the long-chain fatty acid sites is involved in the binding of curcumin to HSA. It is surprising, however, that both ibuprofen and warfarin,

having distinct primary binding sites, show competition with curcumin. According to the 0.72 : 1 stoichiometry of the curcumin–HSA complex, there is no reason to assume that curcumin binds to both sites I and II. Furthermore, if curcumin would bind to site II in subdomain IIIA addition of diazepam should be much more effective than found in the experiment. Two additional experimental facts must also be taken into account:

- (a) X-Ray structures proved palmitic acid binds to both main drug-binding sites of HSA;⁴³
- (b) Ibuprofen has secondary binding sites on HSA^{48,49} and it shows a definite displacing effect on HSA-bound bilirubin,⁵⁰ the latter being bound somewhere in domain II.^{9,41}

In conclusion, these data suggest that the primary binding site of curcumin is located in domain II of HSA and that site I, the deep hydrophobic cavity of subdomain IIA, is presumably involved in curcumin binding.

2.7. Fluorescence spectroscopic investigation of curcumin–HSA interaction at pH 9

A single tryptophan residue, Trp214, located in the depth of subdomain IIA is largely responsible for the intrinsic fluorescence of HSA. As a participant in the formation of the wall of the binding cavity (site I), fluorescence quenching of Trp214 is a sensitive indicator of the binding of a ligand molecule to this site. Measured in pH 7 Tris–HCl buffer, Reddy et al. reported that fluorescence of HSA decreased by 25% at a curcumin concentration of 5.8×10^{-6} M ($C_{\text{HSA}} = 1.13 \times 10^{-6}$ M, L/P=5.1).⁴ Our fluorescence spectroscopic measurements performed in 0.1 M pH 9 Tris–HCl buffer solution indicated that curcumin quenches the fluorescence of HSA more effectively than at pH 7; intrinsic fluorescence of HSA decreased by $\approx 80\%$ at L/P value of 4.55 (Fig. 10). These results suggest that both neutral and dissociated forms of curcumin are bound in the vicinity of Trp214, i.e. at site I. Ionized ligand molecules, however, bind more tightly to this site probably due to the altered secondary interactions between curcumin and HSA residues. Additionally, neutral curcumin molecules associate to subdomain IIA in a nearly linear conformation (weak induced CD spectrum at pH 7 and 7.4^{4,5}) while at pH 9 they bind in a non-planar conformation that is responsible for the bisignate CD spectrum.

2.8. Automated docking of curcumin molecule to HSA for mapping its potential binding sites

Before the docking procedure, the enol form of neutral curcumin molecule was optimized by semiempirical quantum-chemical method (AM1). This procedure was followed in order to avoid the excessive effect of the electrostatic term. Randomly oriented ligand molecules were the subjects for docking calculations performed using the crystal structure of HSA taken from the Protein Data Bank (entry PDB code 1BMO). According to the best energy ranked results shown in Figure 11, all domains have potential binding sites for cur-

cumin. In domains I and II docked curcumin molecules are positioned according to palmitic acid binding sites determined crystallographically. It should be mentioned that the docking procedure did not place ligand molecule within subdomain IIIA where site II and two palmitic acid binding sites are located. At subdomains IIIB and at the interface between subdomains IIA and IIB the ligand molecules are bound superficially in shallow hydrophobic clefts exposed to solvent molecules. Since above pH 7 curcumin is very unstable, these protein sites seem unsuitable to protect their ligand against hydrolytic degradation. From this point of view, the deep drug-binding pocket in subdomain IIA (site I) is much favoured. The two halves of curcumin molecule found in this cavity are rotated relative to each other around the central methine bridge (Fig. 12). The intramolecular hydrogen bond is broken up

and the oxygen atoms point to opposite directions. Since long axes of the two feruloyl parts form a positive dihedral angle ($+156^\circ$), this chiral (right handed) conformation of the curcumin molecule might be responsible for the induced CD exciton couplet. As shown in Figure 13, several amino acid residues are found to be important in forming the binding environment of this ligand molecule. Basic amino acids like Lys199 and Arg218 are in suitable positions to be involved in making H-bonds with the carbonyl oxygen functions at the center of the molecule. The binding might be further stabilized by forming intermolecular H-bonds between Ser287, Arg257, Lys286 and the phenolate groups of curcumin. Some aliphatic amino acids such as Leu238, Leu260, Ala291 and Ala215 containing non-polar side chains also interact with the hydrophobic/aromatic moieties of curcumin. It is noteworthy that

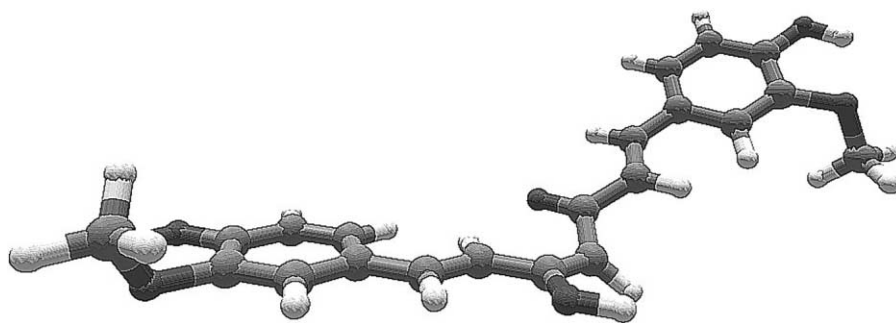


Figure 12. Structure of the docked curcumin molecule found at site I of HSA. Electronic transition moments are polarized along the long axes of feruloyl chromophores. Dihedral angle between the transition moments is $+156^\circ$.

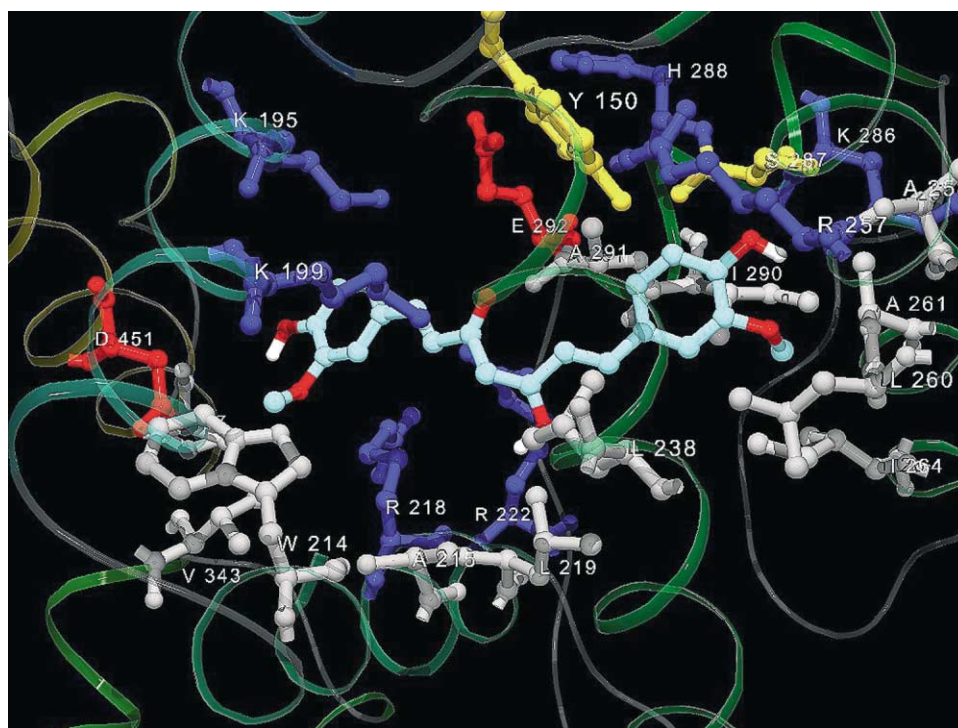


Figure 13. Protein microenvironment of the curcumin molecule (carbon, light blue; oxygen, red; hydrogen, white) in the hydrophobic cavity of subdomain IIA (site I) obtained by the docking procedure. Designated by their one letter amino acid codes, HSA residues found within 5 Å range of the ligand molecule are shown in ball-and-stick representation.

the single tryptophan residue of HSA (Trp214) is also in the immediate environment of the docked curcumin molecule. Our modelling calculations showed that site I has enough room to accommodate curcumin molecule in extended, linear conformation as well.

3. Conclusions

Novel findings of this work are as follows:

- Acid dissociation of the phenolic hydroxyl group in the *para* position dramatically changes light absorption properties of half-curcumin and curcumin causing a large red shift of their main absorption band. Additionally, deprotonation of the second phenolic and the enolic OH substituents of curcumin play only a secondary role in the absorption spectral changes.
- The intact diarylheptanoid structure is essential to obtain the induced exciton CD spectra of curcumin–HSA complex.
- Dissociation of the first phenolic OH group of curcumin is an important step in developing the bisignate CD spectrum.
- Calculated from pH dependent CD spectra, the first pK_a value of curcumin is found to be 8.28. Based on the analysis of CD and absorption spectra of HSA-bound curcumin, it is assigned to the acid dissociation of the first phenolic hydroxyl group.
- The effect of intramolecular exciton coupling on the absorption spectrum of HSA-bound curcumin, and the spectral contributions of neutral and ionized curcumin species have been demonstrated.
- Results of fluorescence quenching measurements and CD displacement experiments using marker ligands of HSA suggested the binding site of curcumin to be located in the hydrophobic pocket of subdomain IIA.
- Molecular modelling calculations showed that curcumin binds near the single tryptophan residue of HSA in a right-handed conformation stabilized by a number of basic amino acids able to form intermolecular hydrogen bonds.

4. Materials and methods

4.1. Materials

Essentially fatty acid free human (HSA) and rabbit serum albumins (RSA) (Sigma, catalog No. A-1887 and A-9438), curcumin (Sigma, catalog No. C-7727) and dehydrozingerone (4-(4-hydroxy-3-methoxyphenyl)-3-buten-2-one or half-curcumin, Aldrich, catalog No. 30604-5) were used as supplied. Palmitic acid (P-5585), *rac*-warfarin and crystalline bilirubin (B4126, 88% bilirubin IX α , 7% bilirubin III α , 5% bilirubin XIII α) were purchased from Sigma and were used without further treatment. Diazepam was the gift of Chemical Works of Gedeon Richter Ltd., Budapest. *rac*-Ibuprofen was obtained from ANDENO B.V. (The Netherlands). Double distilled water, HPLC grade ethanol (Chemolab, Hungary) and spectroscopy grade dimethyl

sulfoxide (DMSO, Scharlau Chemie S.A., Barcelona, Spain) were used. All other chemicals were of analytical grade.

4.2. Preparation of HSA solutions

For spectroscopic sample preparation, HSA was dissolved in a pH 7.4 Ringer or pH 9.0 Tris (0.1 M) buffer solutions. Albumin concentration was calculated with the value of $E_{1\%}^{1\text{cm}} = 5.31$ using experimentally obtained absorbance data at 279 nm.⁹ Molecular weight of HSA was taken to be 66,500.

4.3. Preparation of curcumin stock solution

Curcumin was dissolved in 100% ethanol; the concentration was measured by determining light absorption at the λ_{max} ($\epsilon_{429\text{ nm}} = 55,000\text{ M}^{-1}\text{ cm}^{-1}$).^{1,10}

4.4. Circular dichroism and UV–vis absorption spectroscopy

CD and absorption spectra were recorded on a Jasco J-715 spectropolarimeter in a rectangular cuvette with 1 cm optical pathlength. Temperature control was provided by a Peltier thermostat equipped with magnetic stirring. All spectra were accumulated four times with a bandwidth of 1.0 nm and a resolution of 0.2 nm at a scan speed of 100 nm/min. Induced CD is defined as the CD of curcumin–HSA mixture minus the CD of HSA alone at the same wavelengths and is expressed as ellipticity in millidegrees (mdeg).

4.5. UV–vis absorption spectra of half-curcumin (hC) and curcumin in ethanolic solution with and without added KOH

$2.3 \times 10^{-5}\text{ M}$ and $3.0 \times 10^{-5}\text{ M}$ curcumin and hC ethanolic solutions were prepared and measured between 210 and 550 nm in a rectangular cuvette with 1 cm optical pathlength (room temperature). Then 20–20 μl 0.1 M KOH were added to both samples and the absorption spectra were taken again between 210 and 720 nm.

4.6. CD–pH titration of curcumin solution in the presence of HSA

0.35 ml ethanolic ligand solution ($c = 2.0 \times 10^{-3}\text{ M}$) was added to 14.2 ml of a $4.8 \times 10^{-5}\text{ M}$ HSA solution prepared in double distilled water. After measuring the pH (6.91) 2 ml was placed in a rectangular cuvette with 1 cm optical pathlength and the CD and absorption spectra were registered. Then, μl volumes from 0.01 and 0.1 M NaOH solution were pipetted consecutively to achieve pH 6.91, 7.38, 7.68, 7.97, 8.31, 8.57, 8.78, 9.00 and 9.32, respectively, and the spectra were measured at each pH value (room temperature). For pH measurements a digital pH meter (Radelkis, Budapest) with a combined glass electrode was used.

4.7. CD and UV–vis spectra of half-curcumin in the presence of HSA

2×10^{-3} M stock solution of the ligand was prepared by dissolving 0.087 mg hC in 2.26 ml EtOH. 60–60 μ l stock solution was added to 2 ml HSA solution made in 0.1 M pH 9.0 Tris buffer, or pH 7.4 Ringer buffer ($c_{\text{hC}} = 5.8 \times 10^{-5}$ M, $c_{\text{HSA}} = 9.7 \times 10^{-5}$ M, L/P=0.6, $t = 20^\circ\text{C}$). Spectra were measured between 300 and 550 nm.

4.8. CD and UV–vis spectra of curcumin–HSA, bilirubin–HSA and bilirubin–RSA complexes

30 μ l volume of curcumin ethanolic stock solution was added to 2 ml HSA solution prepared in 0.1 M pH 9.0 Tris–HCl buffer and CD/UV–vis spectra were measured between 300 and 600 nm ($c_{\text{curcumin}} = 3 \times 10^{-5}$ M, $c_{\text{HSA}} = 1 \times 10^{-4}$ M, L/P=0.3, $t = 20^\circ\text{C}$). Bilirubin was dissolved in 0.1 M KOH to obtain 2×10^{-3} M stock solution; from this 30 μ l was added to 2 ml HSA or 2 ml rabbit serum albumin solution prepared in pH 7.4 Ringer buffer. Spectra were taken between 300 and 560 nm ($c_{\text{bilirubin}} = 3 \times 10^{-5}$ M, $c_{\text{HSA}} = c_{\text{RSA}} = 1 \times 10^{-4}$ M, L/P=0.3, $t = 20^\circ\text{C}$).

4.9. Measurements of CD and UV–vis spectra of curcumin–HSA solutions with added site-marker ligands of HSA

CD and UV–vis measurements were made in 0.1 M pH 9 Tris–HCl buffer using 1 cm cell at 37°C . Stock solutions of the ligands were prepared as follows and added stepwise in μ l volumes to the curcumin–HSA solutions: 8×10^{-3} M palmitic acid, 1.2×10^{-2} M *rac*-ibuprofen and 8×10^{-3} M diazepam in EtOH; 6.8×10^{-3} M *rac*-warfarin in 0.1 M Tris–HCl buffer, pH 9 (ethanol concentration never exceeded 13% and the effects of the organic solvent on the CD measurements were undetectable). HSA solutions were 4.9×10^{-5} M for palmitic acid, *rac*-ibuprofen, *rac*-warfarin measurements and 5.5×10^{-5} M for the experiments with diazepam. In all cases curcumin concentration was 2.5×10^{-5} M ([curcumin]/[HSA]=0.50 and 0.45 for diazepam). Molar ratios of marker ligands/HSA (m/HSA) and marker ligands/curcumin (m/curcumin) were changed as follows: palmitic acid, m/HSA 0.40–5.6, m/curcumin 0.80–11.2; *rac*-ibuprofen, m/HSA 0.6–10.2, m/curcumin 1.2–20.4; diazepam, m/HSA 0.2–10.3, m/curcumin 0.5–23.0.

4.10. Measuring the intrinsic fluorescence of HSA in the presence of curcumin

2 ml 4.4×10^{-6} M HSA solution was prepared in a 1 cm rectangular cell by 0.1 M pH 9 Tris–HCl buffer. 5.0×10^{-4} M ethanolic curcumin solution in μ l volumes were consecutively added to the cuvette placed in the sample chamber of the Jasco J-715 spectropolarimeter. Sample solution was excited between 240 and 360 nm with 0.2 nm wavelength steps. Total fluorescence intensity was collected at each wavelength by a Hamamatsu H5784 type photomultiplier detector mounted on a right angle to the light source.

In the sample solution, initial and final concentrations of HSA and curcumin were 4.4×10^{-6} M– 4.1×10^{-6} M and 5.0×10^{-7} M– 3.9×10^{-5} M, respectively. Curcumin/HSA molar ratio was varied between 0.11 and 9.66. During the fluorescence measurements, ethanol concentration did not exceed 10 v/v%. Control experiments performed with albumin and EtOH proved the effect of the organic solvent to be undetectable on the fluorescence of HSA.

4.11. Quantum-chemical calculations and molecular modelling

Geometry optimization of 4-phenyl-3-buten-2-one and curcumin molecules was carried out by Gaussian 98 program using AM1 semiempirical method. Gaussview program was utilized to visualise calculated HOMO and LUMO orbitals. MOS-F semiempirical package with WinMopac interface was used in excited state calculations. Atomic charge densities in first excited states were calculated by the CNDO/S3 method.

Autodock 3.0 program package¹¹ was used for mapping the energetically most favourable binding of neutral curcumin to the crystal structure of HSA (Protein Data Bank code: 1BMO). Gasteiger–Huckel partial charges were applied both for curcumin and protein. Solvation parameters were added to the protein coordinate file and the ligand torsions were defined using the ‘Addsol’ and ‘Autotors’ utilities, respectively. The atomic affinity grids were prepared with 0.375 Å spacing by the Auto-grid program using three $33.75 \times 45 \times 30$ Å boxes, which include the whole protein target. Random starting positions, orientations and torsions (for flexible bonds) were used for the ligand; each docking run consisted of 100 cycles.

Acknowledgements

Financial support from the National R&D Fund (1/047 NKFP Medichem), from the European Community (QLK2-CT-2002-90436), and from the National Fund for Scientific Research (OTKA T33109) are gratefully acknowledged.

References

- Govindarajan, V. S. *CRC Cr. Rev. Food. Sci.* **1980**, *12*, 199–301.
- Khanna, N. M. *Curr. Sci. India* **1999**, *76*, 1351–1356.
- Krishnaswamy, K.; Raghuramulu, N. *Indian J. Med. Res.* **1998**, *108*, 167–181.
- Miquel, J.; Bernd, A.; Sempere, J. M.; Diaz-Alperi, J.; Ramirez, A. *Arch. Gerontol. Geriatr.* **2002**, *34*, 37–46.
- Reddy, A. C. P.; Sudharshan, E.; Rao, A. G. A.; Lokesh, B. R. *Lipids* **1999**, *34*, 1025–1029.
- Zsila, F.; Bikádi, Z.; Simonyi, M. *Biochem. Biophys. Res. Commun.* **2003**, *301*, 776–782.
- Aggarwal, B. B.; Kumar, A.; Bharti, A. C. *Anticancer Res.* **2003**, *23*, 363–398.

8. Began, G.; Sudharshan, E.; Rao, A. G. A. *Lipids* **1998**, *33*, 1223–1228.
9. Peters, T. *All About Albumin: Biochemistry, Genetics and Medical Applications*; Academic Press: San Diego, 1996; p. 25.
10. Jasim, F.; Ali, F. *Microchem. J.* **1989**, *39*, 156–159.
11. Morris, G. M.; Goodsell, D. S.; Halliday, R. S.; Huey, R.; Hart, W. E.; Belew, R. K.; Olson, A. J. *J. Comp. Chem.* **1998**, *19*, 1639–1662.
12. Chignell, C. F.; Bilski, P.; Reszka, K. J.; Motten, A. G.; Sik, R. H.; Dahl, T. A. *Photochem. Photobiol.* **1994**, *59*, 295–302.
13. Griffiths, J. *Colour and Constitution of Organic Molecules*; Academic Press: New York, 1976.
14. Verdine, G. L.; Nakanishi, K. *J. Chem. Soc., Chem. Commun.* **1985**, *16*, 1093–1095.
15. Wiesler, W. T.; Vazquez, J. T.; Nakanishi, K. *J. Am. Chem. Soc.* **1987**, *109*, 5586–5592.
16. Lemon, H. W. *J. Am. Chem. Soc.* **1947**, *69*, 2998–3000.
17. Jurd, L. *Arch. Biochem. Biophys.* **1956**, *63*, 376–381.
18. Aulin-Erdtman, G.; Sandén, R. *Acta Chem. Scand.* **1968**, *22*, 1187–1209.
19. Tonnesen, H. H.; Karlsen, J.; Mostad, A. *Acta Chem. Scand. B* **1982**, *36*, 475–479.
20. Roughley, P. J.; Whiting, D. A. *J. Chem. Soc., Perkin Trans. 1* **1973**, 2379–2388.
21. Arrieta, A.; Beyer, L.; Kleinpeter, E.; Lehmann, J.; Dargatz, M. *J. Prakt. Chem.* **1992**, *334*, 696–700.
22. Khopde, S. M.; Priyadarsini, K. I.; Palit, D. K.; Mukherjee, T. *Photochem. Photobiol.* **2000**, *72*, 625–631.
23. Bong, P. H. *Bull. Korean Chem. Soc.* **2000**, *21*, 81–86.
24. Balasubramanian, K. *Indian J. Chem. A* **1991**, *30*, 61–65.
25. Dietze, F.; Arrieta, A. F.; Zimmer, U. *Pharmazie* **1997**, *52*, 302–306.
26. Borsari, M.; Ferrari, E.; Grandi, R.; Saladini, M. *Inorg. Chim. Acta* **2002**, *328*, 61–68.
27. Tonnesen, H. H.; Karlsen, J. *Z. Lebensm. Unters. Forsch.* **1985**, *180*, 402–404.
28. Tonnesen, H. H.; Karlsen, J. *Z. Lebensm. Unters. Forsch.* **1985**, *180*, 132–134.
29. Wittmann, H.; Uragg, H.; Sterk, H. *Mh. Chem.* **1966**, *97*, 896–904.
30. Dyrssen, D. W.; Novikov, Y. P.; Uppström, L. R. *Anal. Chim. Acta* **1972**, *60*, 139–151.
31. Tang, B.; Ma, L.; Wang, H.; Zhang, G. *J. Agric. Food Chem.* **2002**, *50*, 1355–1361.
32. Merdy, P.; Guillon, E.; Aplincourt, M.; Duomonceau, J. *J. Chem. Res. S* **2000**, 76–77.
33. Harada, N.; Nakanishi, K. *Circular Dichroic Spectroscopy–Exciton Coupling in Organic Stereochemistry*; University Science Books: California, 1983.
34. Pedersen, U.; Rasmussen, P. B.; Lawesson, S.-O. *Liebigs Ann. Chem.* **1985**, 1557–1569.
35. Bos, O. J. M.; Labro, J. F. A.; Fischer, M. J. E.; Wilting, J.; Janssen, L. H. M. *J. Biol. Chem.* **1989**, *264*, 953–959.
36. Era, S.; Itoh, K. B.; Sogami, M.; Kuwata, K.; Iwama, T.; Yamada, H.; Watari, H. *Int. J. Pept. Prot. Res.* **1990**, *35*, 1–11.
37. Dockal, M.; Carter, D. C.; Ruker, F. *J. Biol. Chem.* **2000**, *275*, 3042–3050.
38. Kasaimorita, S.; Horie, T.; Awazu, S. *Biochim. Biophys. Acta* **1987**, *915*, 277–283.
39. Kosa, T.; Maruyama, T.; Sakai, N.; Yonemura, N.; Yahara, S.; Otagiri, M. *Pharmaceut. Res.* **1998**, *15*, 592–598.
40. Blauer, G. *Israel J. Chem.* **1983**, *23*, 201–209.
41. Petersen, C. E.; Ha, C.-E.; Harohalli, K.; Feix, J. B.; Bhagavan, N. V. *J. Biol. Chem.* **2000**, *275*, 20985–20995.
42. Blauer, G.; Wagniere, G. *J. Am. Chem. Soc.* **1975**, *97*, 1949–1954.
43. Curry, S.; Brick, P.; Franks, N. P. *Biochim. Biophys. Acta* **1999**, *1441*, 131–140.
44. Carter, D. C.; Ho, J. X. *Adv. Protein Chem.* **1994**, *45*, 153–203.
45. Sugio, S.; Kashima, A.; Mochizuki, S.; Noda, M.; Kobayashi, K. *Protein Eng.* **1999**, *12*, 439–446.
46. Petitpas, I.; Bhattacharya, A. A.; Twine, S.; East, M.; Curry, S. *J. Biol. Chem.* **2001**, *276*, 22804–22809.
47. Itoh, T.; Saura, Y.; Tsuda, Y.; Yamada, H. *Chirality* **1997**, *9*, 643–649.
48. Fitos, I.; Visy, J.; Simonyi, M.; Hermansson, J. *Chirality* **1999**, *11*, 115–120.
49. Dockal, M.; Carter, D. C.; Ruker, F. *J. Biol. Chem.* **1999**, *274*, 29303–29310.
50. CooperPeel, C.; Brodersen, R.; Robertson, A. *Pharmacol. Toxicol.* **1996**, *79*, 297–299.